Bioimages 4 (2): 73–78, June 1996.

SEM Imaging of Single Heavy Meromyosin Molecules on Hydrophilic Silicon Surface

Taiji Furuno[1]*, Hidetake Miyata[2], Hiroshi Yoshikawa[2], Kazuhiko Kinosita Jr.[2], Akira Ikegami[1], Hiroyuki Sasabe[3] and Wolfgang Knoll[3]

[1]Department of Physics, School of Medicine, [2]Department of Physics, Faculty of Science and Technology, Keio University, Hiyoshi, Kouhoku-ku, Yokohama, Kanagawa 223, Japan, [3]Frontier Research Program, The Institute of Physical and Chemical Research (RIKEN), Hirosawa, Wako, Saitama 351-01, Japan.

Abstract

The fine structure of skeletal muscle heavy meromyosin (HMM) with two heads connected to a thin tail was clearly imaged with a high-resolution scanning electron microscope (SEM) by negative staining on a hydrophilic silicon surface. The single molecular image of HMM was analyzed. A structural change in the HMM head on binding of adenosine triphosphate (ATP) was detected. The HMM molecules with head(s) bent at 6–8 nm from the head-tail junction directed toward the end of the tail were found frequently in the presence of ATP. The estimated value for the bending angle was about 20° on average.

Key words

Electron microscopy, negative staining, muscle, adsorption

Introduction

Protein assemblies on solid surfaces are interesting in both basic and applied studies. In motility assays of motor proteins, myosin molecules are bound to the modified solid surfaces, forming an assembly which drives an actin filament in the presence of ATP (Harada et al., 1990; Kron et al., 1991; Miyata et al., 1994). The protein molecules are sometimes bound to patterned solid surfaces (Mazzola and Fodor, 1995; Matsuda and Sugawara, 1995). Information on the structure of protein assembly is valuable in these studies. When the assemblies are formed on thick plates they must be replicated for examination by transmission electron microscopy (TEM), as has been shown for the myosin molecules bound to the mica surface (Harada et al., 1990). The recently developed atomic force microscopy has a high potential for obtaining molecular images of proteins. However, atomic force microscopy is still not routinely applicable to imaging protein molecules at nanometer resolution. The scanning electron microscopy (SEM) used heretofore to observe large biological structures is capable of imaging single protein molecules. They are observed on a carbon plate by applying sophisticated procedures for specimen preparation (Nakadera et al., 1991). We have shown previously that the negative staining conventionally used in TEM studies is a quick and reliable method also in SEM to observe two-dimensional arrays of protein on a silicon wafer (Furuno et al., 1992; Furuno and Sasabe, 1993; for negative staining see, e.g., Bremer et al., 1992). The present study clearly shows that high-resolution SEM is capable of revealing the shape of single protein molecules.

In the present study we chose skeletal muscle heavy meromyosin (HMM). Information on the structure and structural changes of myosin is important for understanding the molecular mechanism of muscle contraction. The shape and flexibility of the myosin head has been extensively studied by TEM. Specimens were prepared by shadow replication on mica (Elliot and Offer, 1978; Flicker et al., 1983) and by negative staining with special care for carbon support (Walker et al., 1985; Walker and Trinick, 1989). Recent X-ray crystallography has revealed the crystal structure of the myosin head at atomic resolution (Rayment et al., 1993). The structural change of the head upon binding of ATP has been detected by small-angle X-ray scattering as changes in the real-space parameters under physiological conditions (Wakabayashi et al., 1992). The corresponding structural change has also been detected in the present study by measuring the angles at the head portion of HMM.

Materials and Methods

Protein

Chymotryptic heavy meromyosin (HMM) was prepared from rabbit skeletal muscle as previously described (Weeds and Pope, 1977; Spudich and Watt, 1971). HMM was stored in aliquots in liquid nitrogen (8 mg/ml, 10 mM-MOPS, pH 7.0, 2 mM-$MgCl_2$, 0.6

*To whom all correspondence should be addressed.
E-mail: furuno@cc.hc.keio.ac.jp

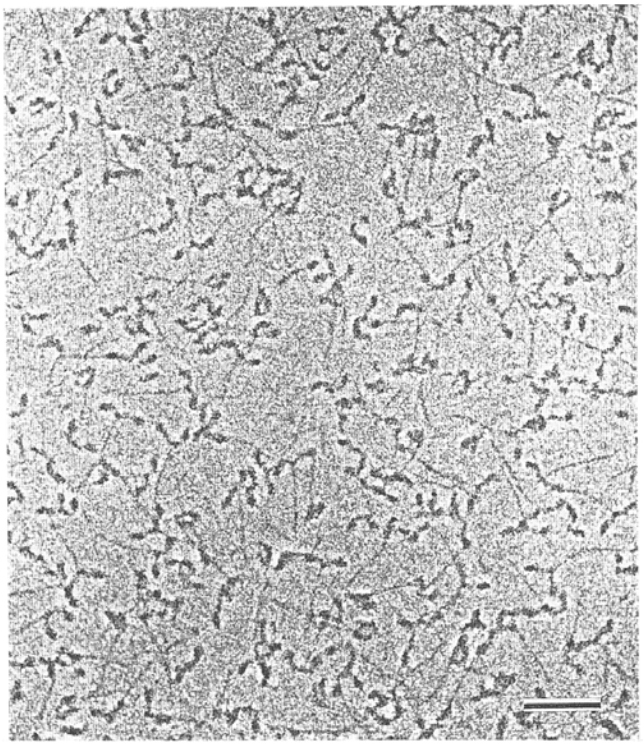

Fig. 1. Scanning electron micrograph of negatively stained HMM molecules on a hydrophilic silicon wafer. The concentration of HMM in the staining solution was 60 μg/ml. The hydrophilic silicon surface was spin-coated with this solution. The direct magnification was ×200,000, at which the raster interval of the SEM primary beam was 3Å, corresponding to half the diameter of an ideally focused electron beam ~6Å. The bar represents 50 nm.

M-KCl, 2 mM-DTT). The activity of the molecules was assayed by in vitro motility (Miyata et al., 1994).

Negative staining and electron microscopy

A chip of silicon wafer (~6×9 mm^2) was used as substrate. It was cleaned in an ultrasonic cleaner (40 kHz frequency) for a few minutes with a neutral detergent (Clean Ace Neutral, Iuchi, Japan). To obtain a hydrophilic surface it was then irradiated in air with a low-pressure mercury lamp (40 W, Sen Light Co., Japan) for 3 min. The hydrophilicity of the silicon surface was saturated after 2 min of irradiation under our shining condition. The HMM specimens were prepared on this fully hydrophilic silicon surface.

The negatively stained specimens were prepared by a method similar to that reported previously (Furuno and Sasabe, 1993). Methylamine tungstate (MAT, Agar Scientific Ltd., UK) was used as the stain. The MAT solution was filtered before use with a molecular filter (UFP2-TTK, Nihon Millipore Ltd.). A drop (~8 μl) of MAT solution (2.5%, pH 7.1 adjusted with KOH) containing HMM (10–1000 μg/ml) was spread on the silicon surface. The wafer was placed in an Eppendorf tube (1.5 ml) and spun with a micro-centrifuge at 6000 rpm (45° fixed-angle, ~4 cm rotational radius at the wafer position, 2000×g) with the wet face down for 2–3 s (we refer to this method as spin-coat negative staining). The spin-coat negative staining has the advantage that the staining solution spreads uniformly on the silicon surface as a thin layer due to the centrifugal force which acts obliquely to the silicon face. The normal component of the centrifugal force helps press the solution to the wafer surface, and the parallel one makes it flow and thin to a thickness representing interference fringes. When the wafer is removed from the tube, the surface is instantly dried.

The central part (3×6 mm^2) of the wafer chip was used for imaging with an SEM (S-900, Hitachi Co. Ltd., Japan). The chip was fixed in a specimen-heating holder and kept at 80°C to reduce contamination deposition on the surface during electron beam scan (Furuno et al., 1992). The acceleration voltage was 30 kV, and the electron dose was about 8×10^4 e$^-$/nm^2, which was a similar amount to that applied in TEM studies for high-contrast imaging of the negatively stained myosin (Walker et al., 1985; Walker and Trinick, 1989). The images were recorded on negative films (Neopan F, Fuji Film Co., Japan).

Results and Discussion

Structure of the HMM on the hydrophilic silicon surface

(a) In the absence of ATP

Figure 1 shows a typical SEM image of the HMM molecules. In Fig. 2(b), HMM molecules are arranged consecutively in terms of the angle α between the long axes of the two heads (see Fig. 2(a)). The shape of the HMM head is classified roughly into two forms, a curved head and a straight one (Fig. 2(a)). The shape of the curved heads in Fig. 2(b) resembles that elucidated by X-ray crystallography (Rayment et al., 1993). The length L (see Fig. 2(a)) of the curved head was estimated to be 14–17 nm (mean 15.5 nm), and that for the straight one was 17–20 nm (mean 17.5 nm). The length of the crystal head (16.5 nm) is therefore intermediate between the two.

One or both heads in the first row (Fig. 2(b)) appear curved, and the angle α is $\geq$180°. Both heads are nearly straight in the second row in Fig. 2(b), with the angle α between 135° and 180°. The straight-heads HMM takes an angular range of α between 90° and 180° (2nd and 3rd rows in Fig. 2(b)), appearing as T- or Y-shaped. About 55% of the heads were assigned to this straight shape. The distribution of the angle α is shown in Fig. 3 (filled circles). Although a strict definition and measurement of angle α was difficult, the quality of the molecular images allowed estimation of

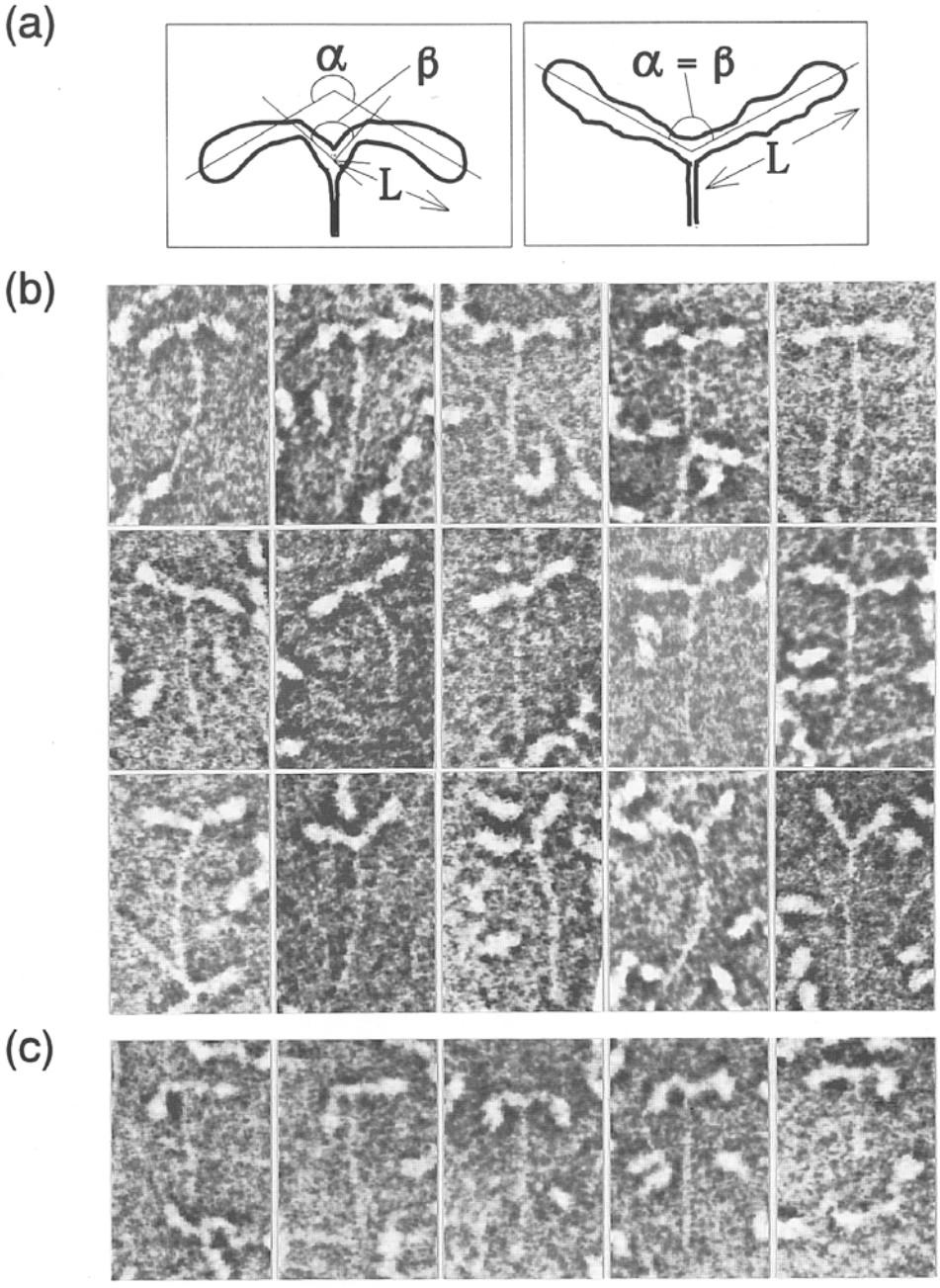

Fig. 2. Gallery of the HMM molecules. The image of each molecule was captured from black and white prints using a CCD camera connected to a personal computer. The brightness and contrast is reversed from the original print, resulting in a bright image of the protein molecule. Noise filtering was not applied.

(a) Schematic representations for the HMM molecules of both-curved and both-straight heads. α indicates the angle spanned by two long axes of the heads, and β the angle between the neck portions joining together to the head-tail junction.

(b) SEM images of HMM negatively stained in the absence of ATP. The images are arranged according to the angle α, decreasing from left to right , top to bottom.

(c) The HMM images exhibiting typical bending of the head(s) in the presence of Mg-ATP. Equivolume of HMM (1.0 mg/ml, 12 mM imidazole, 90 mM KCl, 2.5 mM $MgCl_2$, pH 7.4) and ATP (2 mM, pH 7.0) solutions were mixed together just before being diluted to 50–70 μg/ml with MAT. The negatively stained specimen was prepared within 2 min after the mixing. Magnification is $\times$400,000 for Figs. 2(b) and (c).

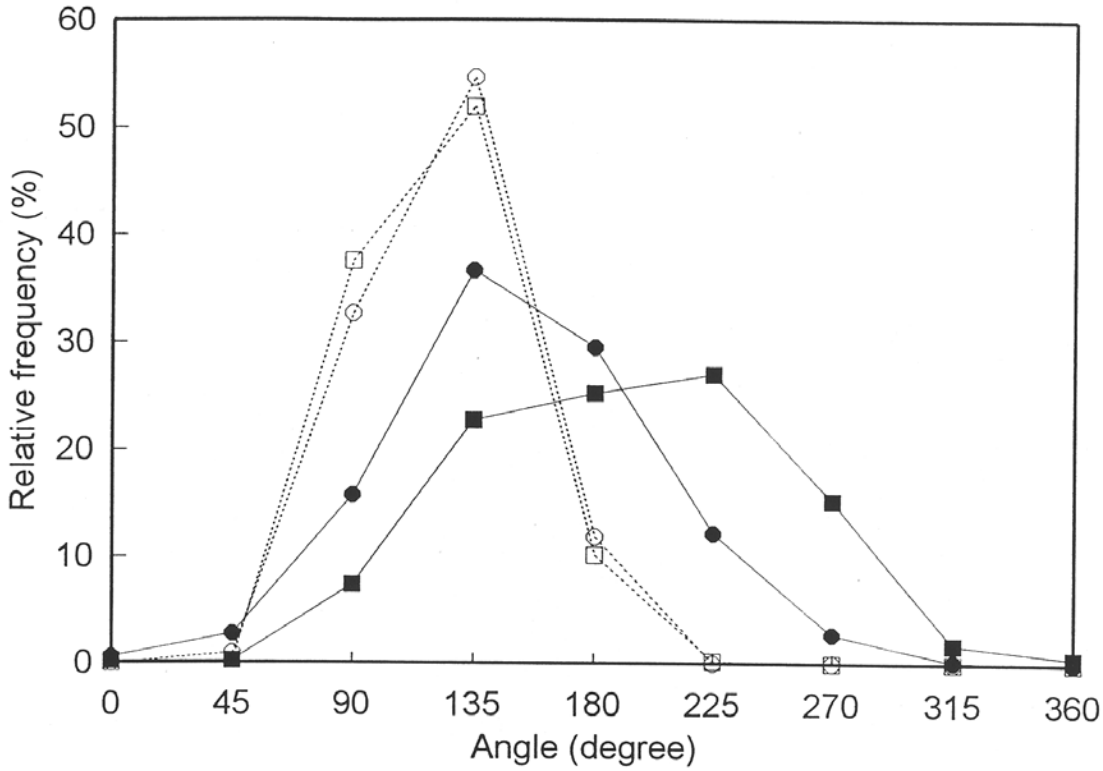

Fig. 3. Distribution of the two angles of α and β which characterize the shape of the HMM molecule. The distribution was obtained by visual inspection of α at the angular resolution of 45° without ATP (filled circle, n=520) and with ATP (filled square, n=440). The average value of α was 153° and 192°, respectively. The angle β was also determined similarly without ATP (open circle, n=420) and with ATP (open square, n=420). The average values were 125° and 123° with and without ATP respectively. Molecules well isolated from others were selected randomly for the above inspection. Some of the molecules selected for the evaluation of α were excluded for the evaluation of β because they were unclear at the neck portion.

α visually at an angular resolution of 45° (half of a right angle). Later we will discuss the distribution of α in conjunction with the structural changes of the head in the presence of ATP.

The angle β at the head-tail junction, where the neck portion of each head joins the tail (see Fig. 2(a)), seems to be confined to a narrow range between 90° and 180° (open symbols in Fig. 3). The average of angle β was 125°. The head-tail junction therefore seems to be sufficiently rigid or elastic to be resistant against forces exerted during negative staining on the wafer. This result is in contrast to the previous TEM studies (Elliot and Offer, 1978; Walker and Trinick, 1989), where flexibility of the head-tail junction was concluded.

Walker et al. (1985) found that clockwise curvature of the myosin head was the most common type on the carbon support, and concluded that there was a preferred affinity of one side of the HMM head to the carbon surface. We undertook a similar analysis to characterize the affinity of the myosin head to the hydrophilic silicon surface. In our study, most of the curved right heads showed a clockwise curvature while the left heads curved counterclockwise when viewed from the head-tail junction to the remote end of the head. This suggests that the myosin head interacts with the hydrophilic silicon wafer in a weaker manner than with the carbon film. Thus the silicon surface might be more suitable for preserving protein molecules.

(b) In the presence of ATP

A structural change in the myosin head induced by binding of nucleotide ATP has been detected in the present study. The increase in the angle α in the presence of ATP is clearly shown in the distribution curves in Fig. 3 (filled symbols). The percentage of the molecules with highly curved or bent head(s) as shown in Fig. 2(c) was about 12%, while such heads were found in 2–4% of molecules in the absence of ATP. The bending position was at 6–8 nm from the head-tail junction, and the direction of bending was mostly downward, i.e., toward the end of the tail. The bending position found in the present study is closer to the head-tail junction by 4–6 nm than in previously reported by TEM studies of shadow replicas (Tokunaga et al., 1991).

The curving of the head obtained here may correspond to that elucidated by model calculation for the small-angle X-ray scattering of the single head of myosin in solution (Wakabayashi et al., 1992), where

the calculation was carried out assuming monodispersity of the molecular shape. The maximum frequency in the distribution of α increased, as shown in Fig. 3, from 135° to 225°; the increase in the average of α was from 153° to 192°, indicating a bending by 20° per head considering that β was almost unchanged in the presence of ATP (open symbols in Fig. 3). Interestingly, this value of 20° is close to that estimated for the bending angle of the model head in the X-ray solution study (Wakabayashi et al., 1992).

We have thus shown by measuring the angles of α and β that the head-tail junction has a certain stiffness and the HMM head undergoes a conformational change on binding of ATP. The fact that the average of α was larger than that of β indicates again that the head would not freely rotate at the junction; otherwise the average of the angles α and β would be close, while taking different distribution curves.

Advantage and disadvantage of the present SEM technique

The specimen preparation for SEM was easy, as described here, and we obtained clear images of negatively stained HMM reproducibly. However, a number of technical problems were found in the specimen preparation.

The major problem was related to the controlled adsorption of the protein molecules to the silicon surface. HMM molecules were not bound to the fully hydrophilic silicon surface prepared by the deep-UV irradiation, resulting in a slight difficulty in obtaining specimens with uniform and low-density distribution. Especially below a concentration of 30 μg/ml of HMM solution, we rarely found molecules on the silicon surface. At such a concentration range, adsorption of the HMM to the pipette wall and its denaturation at the air/water interface after being spread over the silicon surface would have seriously competed with the deposition by spin-coat negative staining. Even at a higher concentration of slightly below 100 μg/ml, a tendency toward inhomogeneous distribution of HMM was noticed, presumably caused by the flow of staining solution during drying immediately after spinning.

Despite these difficulties, we consider the use of a fully hydrophilic silicon surface essentially important for the high-resolution imaging, since clear images of protein are given on that surface. The surface of a silicon wafer kept in air a long time was slightly hydrophobic, probably due to contamination in the atmosphere. By adjusting the time for UV irradiation we could control to some extent the hydrophilicity of the silicon surface. On a surface with less hydrophilicity the molecules were left bound after rinsing with a buffer, in contrast to the fully hydrophilic silicon surface. However, the molecular images were poor on such sticky surfaces. The observation of the narrow tails of HMM was difficult, and the images of the heads were blurred (data not shown). The results suggest flattening or denaturation on binding to the surface. A hydrophilic silicon surface thus seems to be necessary for obtaining high-resolution images by SEM.

Although the proteins on the wafer should have been damaged at the high electron dose of 8×10^4 e^-/nm^2 which we used for imaging, the molecules were stably imaged at high contrast. Deformation of the protein molecules during SEM observation was not noticed. The use of bulk silicon substrate to which the molecules are bound tightly by negative staining aided in avoiding the thermal problems caused by electron beam irradiation. Rather, the most serious actual problem was the contamination of the surface during imaging, although this problem was reduced considerably by using a specimen-heating holder, as we mentioned previously (Furuno et al., 1992).

Conclusion

The present study demonstrates the ease of both specimen preparation and high-resolution imaging of proteins on a hydrophilic silicon surface. The obtained results confirm the technological importance of the combined use of SEM and negative staining. In addition, valuable information on the structure and structural change in the HMM head is provided. The angle β at the head-tail junction is confined to 90–180° and the heads are symmetrically arranged with respect to the tail, suggesting a certain stiffness of the head-tail junction which may limit completely independent movement of the heads relative to one another. It is clearly shown furthermore that by binding of ATP the head tends to be curved or bent at 6–8 nm from the head-tail junction toward the end of the tail.

Acknowledgment

This research was supported by the Special Coordination Funds for Promoting Science and Technology from the Science and Technology Agency, Japan.

Received May 13, 1996; revised June 28, 1996.

References

Bremer, A., Henn, C., Engel, A., Baumeister, W. and Aebi, U. (1992). Has negative staining still a place in biomacromolecular electron microscopy? Ultramicroscopy, 46: 85–111.

Elliott, A. and Offer, G. (1978). Shape and flexibility of the myosin molecule. J. Mol. Biol., 123: 505–519.

Flicker, P.F., Wallimann, T. and Vibert, P. (1983). Electron microscopy of scallop myosin. Location of

regulatory light chains. J. Mol. Biol., 169: 723–741.
Furuno, T., Ulmer, K.M. and Sasabe, H. (1992). Scanning electron microscopy of negatively stained catalase on a silicon wafer. Microsc. Res. Tech., 21: 32–38.
Furuno, T. and Sasabe, H. (1993). Two-dimensional crystallization of streptavidin by nonspecific binding to a surface film: study with a scanning electron microscope. Biophys. J., 65: 1714–1717.
Harada, Y., Sakurada, K., Aoki, T., Thomas, D.D. and Yanagida, T. (1990). Mechanochemical coupling in actomyosin energy transduction studied by in vitro movement assay. J. Mol. Biol., 216: 49–68.
Kron, S.J., Toyoshima, Y.Y., Uyeda, T.Q.P. and Spudich, J.A. (1991). Assays for actin sliding movement over myosin-coated surfaces. Meth. Enzymol., 196: 399–416.
Matsuda, T. and Sugawara, T. (1995). Development of a novel protein fixation method with micron-order precision. Langmuir, 11: 2267–2271.
Mazzola, L.T. and Fodor, S.P.A. (1995). Imaging biomolecule arrays by atomic force microscopy. Biophys. J., 68: 1653–1660.
Miyata, H., Hakozaki, H., Yoshikawa, H., Suzuki, N., Kinosita, K. Jr., Nishizaka, T. and Ishiwata, S. (1994). Stepwise motion of an actin filament over a small number of heavy meromyosin molecules is revealed in an in vitro motility assay. J. Biochem., (Tokyo) 115: 644–647.
Nakadera, T., Mitsushima, A. and Tanaka, K. (1991). Application of high-resolution scanning electron microscopy to biological macromolecules. J. Micorsc., 163: 43–50.
Rayment, I., Rypniewsky, W.R., Schmidt-Bäse, K., Smith, R., Tomchick, D.R., Benning, M.M., Winkelmann, D.A., Wesenberg, G. and Holden, H.M. (1993). Three-dimensional structure of myosin subfragment-1: a molecular motor. Science, 261: 50–58.
Spudich, J.A. and Watt, S. (1971). The regulation of rabbit skeletal muscle contraction. J. Biol. Chem., 246: 4866–4871.
Tokunaga, M., Sutoh, K. and Wakabayashi, T. (1991). Structure and structural change of the myosin head. Adv. Biophys., 27: 157–167.
Wakabayashi, K., Tokunaga, M., Kohno, I., Sugimoto, Y., Hamanaka, T., Takezawa, Y., Wakabayashi, T. and Amemiya, Y. (1992). Small-angle synchrotron x-ray scattering reveals distinct shape changes of the myosin head during hydrolysis of ATP. Science, 258: 443–447.
Walker, M., Knight, P. and Trinick, J. (1985). Negative staining of myosin molecules. J. Mol. Biol., 184: 535–542.
Walker, M. and Trinick, J. (1989). Electron microscopy of negatively stained scallop myosin molecules. Effect of regulatory light chain removal on head structure. J. Mol. Biol., 208: 469–475.
Weeds, A.G. and Pope, B. (1977). Studies on the chymotryptic digestion of myosin. Effects of divalent cations on proteolytic susceptibility. J. Mol. Biol., 111: 129–157.